Ground-Return Parameters of Submarine Cables Buried in the Seabed

Gianfranco Di Lorenzo, Erika Stracqualursi, *Member, IEEE*, Massimo Marzinotto, *Member, IEEE*, Jose Brandão Faria, *Life Fellow, IEEE*, and Rodolfo Araneo, *Senior Member, IEEE*

***Abstract*—The computation of sea/seabed-return distributed parameters of subsea cables is a relevant topic due to the growing importance of submarine connections. This article presents for the first time new formulas for the computation of self and mutual ground impedances and admittances for submarine cables buried in the seabed. The original theory developed by Sunde is applied to a three-media model with air, sea, and seabed. Referring to the practical installation practice of the Italian transmission system operator Terna S.p.A., we compare the prediction of the available models and assess the effect of the different approximations on the computation of the per unit length ground parameters. Finally, we define the limits of applicability of the available models that differ in accuracy and complexity.**

***Index Terms*—Cable impedance, cable modeling, sea-return impedance, submarine cable.**

Nomenclature

r_i	External radius of cable i.
q_{ij}	Horizontal distance between the directions of cables i and j.
h_s	Sea depth.
h_i	Depth of the cable i axis with respect to the air–water interface.
σ_m	Electric conductivity of the mth layer.
ϵ_m	Electric permittivity of the mth layer.
κ_m	Complex conductivity of the mth layer.
μ_m	Magnetic permeability of the mth layer.
γ_m	Propagation constant of the mth layer.
δ_s	Penetration depth of the sea layer.
$Z'_{m,ii}$, $Y'_{m,ii}$	Per unit length return self-impedance/ admittance of cable i buried in medium m.
$Z'_{m,ij}$, $Y'_{m,ij}$	Per unit length return mutual impedance/ admittance between cables i and j buried in medium m.
$\mathrm{I}_n(\cdot)$, $\mathrm{K}_n(\cdot)$	Modified Bessel function of the first/second kind of order n.

Manuscript received 4 September 2022; revised 7 November 2022, 4 December 2022, and 10 January 2023; accepted 26 January 2023. Date of publication 1 March 2023; date of current version 14 April 2023. *(Corresponding author: Rodolfo Araneo.)*

Gianfranco Di Lorenzo, Erika Stracqualursi, and Rodolfo Araneo are with the Electrical Engineering Division of DIAEE, University of Rome "Sapienza," 00184 Rome, Italy (e-mail: gianfranco.dilorenzo@uniroma1.it; erika.stracqualursi@uniroma1.it; rodolfo.araneo@uniroma1.it).

Massimo Marzinotto is with the Terna S.p.A. (Italian TSO), 00156 Rome, Italy (e-mail: massimo.marzinotto@terna.it).

Jose Brandão Faria is with the Instituto de Telecomunicações, Instituto Superior Técnico, Universidade de Lisboa, 1049-001 Lisboa, Portugal (e-mail: brandao.faria@tecnico.ulisboa.pt).

Color versions of one or more figures in this article are available at https://doi.org/10.1109/TEMC.2023.3241363.

Digital Object Identifier 10.1109/TEMC.2023.3241363

I. Introduction

INSTALLATIONS of submarine (or subsea) cables are growing fast in the recent years. They are widely used in high-voltage dc and ac [1] connections with offshore wind farms [2], wave energy power plants, and offshore petrochemical installations, as well as in the transmission network connections with islands [3] and even continents [4].

Accurate electromagnetic modeling of submarine cables is of crucial importance to insure that, once installed, their performance is robust and meets the design expectations for both the steady state and transient regimes. The analysis of both regimes requires the evaluation/computation of the per unit length (p.u.l.) distributed parameters of the cable to be used in a transmission model, either in frequency [5], [6], [7] or time domain [8]. Additionally, transient analysis needs an accurate computation over a wide frequency range, usually up to a few MHz. At these frequencies, the limits of the quasi-transverse electromagnetic (TEM) approximation are usually encountered for external ground modes in practical cases, since a transition takes place to a surface wave propagation, based on the transverse magnetic Sommerferd–Goubau wave [9].

When dealing with single-core (SC) cables, as is the practical case for dc submarine installations, the p.u.l. impedances relative to the internal layers of a single SC cable can be computed with the coaxial theory developed by Schelkunoff [10], which allows the computation of the interior, exterior, and transfer (or mutual) impedance terms considering the skin effect. The calculation of the p.u.l. admittances is straightforward and does not present any significant difficulty [11]. The effect of the earth-return mode and the intersheath modes supported by the cable system is represented by the external earth-return parameters (i.e., ground impedance and admittance matrices) according to the theory developed in the frequency domain by Pollaczek [12] and later modified by Sunde [13] to include the earth permittivity. A further generalization to the time domain was proposed in [14].

Formulas for the earth impedance and admittance matrices were initially developed in the low-frequency range for

Fig. 1. Submarine cable laying above the water–seabed interface (Courtesy of Nexans).

quasi-TEM propagation, considering two half-spaces, with the top layer being air and the bottom layer being soil (i.e., homogeneous earth model). More advanced theories were proposed in [15], [16], and [17]. A general formulation suitable also in the high-frequency range was developed by Papadopoulos et al. [18]. Then, several efforts were conducted to derive formulas for the inhomogeneous earth case (two-layer earth model): earth-return impedances were computed by Tsiamitros et al. [19] and, later, earth-return admittances were computed by Papadopoulos et al. [20].

Recent contributions on the subject of homogeneous earth were given in [21], where Xue et al. proposed a generalized formulation based on a complete field solution. The theory was used by Salvador et al. [22] to provide a closed-form formula for the ground-return admittance that can be easily used in ATP/EMTP-like simulators. Magalhães et al. [23] showed that the inclusion of the ground-return admittance affects mainly the ground and intersheath modes in shorter cables (length typically below 1 km) buried in highly resistive soils (resistivity typically above a few kΩ·m). Very recently, they also investigated the impact of the ground-return admittance on cross-bonded underground cables in [24]. The authors demonstrated that the ground-return admittance plays a significant role in transient analysis, and its influence cannot be neglected even at a few kilohertz.

The topic of the p.u.l. sea-return parameters of submarine cables (see Fig. 1) has been initially addressed by Bianchi and Luoni [25]. Then, in [26], Lucca used the formulation of Papadopoulos et al. for the two-layer earth to compute the return self and mutual impedances between submarine cables laying on the seabed. In [27], Benato et al. used the infinite-sea model to study the harmonic behavior of HVDC cables. The modeling of cables buried in the seabed was addressed in [28], where Silva et al. used the homogeneous earth model to compute transient simulations. Patel and Triverio also addressed the topic in [29] concerning the applicability of the technique called MOM-SO.

Although not new, the computation of ground-return parameters of buried cables is still a hot topic, as recent contributions show: Papadopoulos et al. investigated how the frequency dependence of the soil properties affects the ground p.u.l. parameters in [30] and [31]; Ghosh and Das [32] developed a generalized approach for underground cables containing N semiconductor screens.

In this article, we propose for the first time new formulas for the computation of the impedance and admittance matrices when the cables are buried in the seabed employing a three-media model air–sea–seabed. This article aims to compare the available models for the computation of the ground-return parameters of submarine cables. Referring to the practical installation practice of the Italian transmission system operator (TSO) Terna S.p.A., the cables are assumed either to lie on the seabed or to be buried in the seabed. We assess the effect of the different approximations on the computation of p.u.l. parameters and we define the limits of applicability of the available models, which differ in accuracy and complexity.

The rest of this article is organized as follows. The main expressions for the self and mutual impedances associated with the ground (seawater) return are presented in Section II, and classified according to the number of layers accounted for in the formulation. In Section III, an expression for the case of cables buried in the seabed is proposed, accounting also for the seawater and air upper layers. Section IV presents and compares numerical results, discussing the effect of different approximations and parameters. Some main relevant remarks are drawn in this section, as well. Finally, in Section V, we conclude this article and provide directions for future research activity.

II. Statement of the Problem and Existing Formulations

The number of layers classifies the available formulations accounted for in the modeling of the half-space below the interface with the air (usually denoted as layer 0). We are interested in double-layer configurations for submarine applications, including the sea (layer 1) and the seabed (layer 2). However, single-layer models will also be discussed as a benchmark for more complex approaches and, depending on the laying conditions of the submarine cables, still representing a solution with acceptable accuracy. The reviewed methods and the proposed formula for the impedances and admittances assume the cables (here, denoted with i and j) to lay horizontally and with parallel axes into the same layer, as from common technical practice.

The installation practice of HVDC submarine cables of the Italian TSO Terna S.p.A. changes with respect to the distance from the coastline. Up to 400 m, the cables are buried at $0.7-1$ m under the seabed surface through jet trenching technology [33] to avoid that trawling or anchoring activities may damage them. Beyond 400 m, the two cables are laid directly on the seabed interface. An exception to this common practice is when Neptune grass is encountered near the coastline; in this case, the cables are laid on the seabed interface, and the jet trenching technology is avoided for environmental reasons.

A. Single-Layer Earth

We will refer to the configuration in Fig. 2(a), in which q_{ij} denotes the horizontal distance between the directions of cables i and j, and depths h_i and h_j are in absolute value. Single-layer formulations were originally derived for underground cables (i.e., for ground–air interface), although they may be extended to the case of sea–air or seabed–sea interfaces for submarine cables applications. Hence, we will generally refer to cables buried in

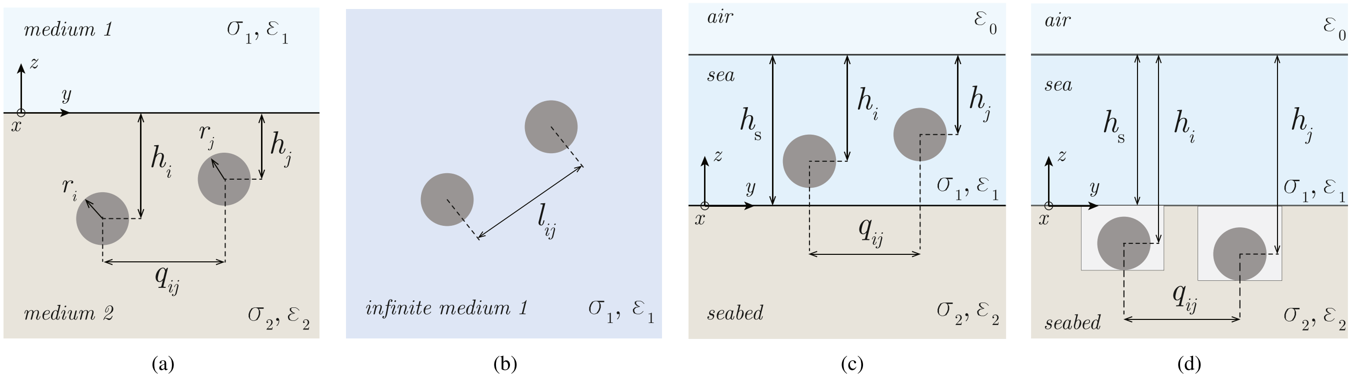

Fig. 2. Geometric details of laying configurations of two insulated submarine cables. (a) Single-layer earth. (b) Infinite-medium model. (c) Double-layer earth, cables in the seawater. (d) Double-layer earth, cables buried in the seabed.

the medium 2 (seabed or sea) with the medium 1 placed above (sea or air—in this latter case denoted as layer 0).

1) Pollaczek–Sunde: The first formula for the ground-return impedances was suggested by Pollaczek [12] who assumed a resistive, homogeneous earth (medium 2) behaving as a conductor, with air placed above (medium 1). His formula, written for medium 2, reads

$$Z'_{2,ij} = \frac{j\omega\mu_2}{2\pi}\left[\mathrm{K}_0\left(\gamma_2 l_{ij}\right) - \mathrm{K}_0\left(\gamma_2 L_{ij}\right) + 2\int_0^\infty \frac{\mathrm{e}^{-2\alpha_2 h_{ij}}}{\lambda+\alpha_2}\cos\left(\lambda\, q_{ij}\right)\,\mathrm{d}\lambda\right] \tag{1}$$

where $h_{ij} = \frac{h_i + h_j}{2}$ and $\alpha_m = \sqrt{\lambda^2 + \gamma_m^2}$. In (1), the integral is known as the Pollaczek's correction integral and the following definitions hold:

$$\begin{aligned} l_{ij} &= \sqrt{q_{ij}^2 + \left(h_i - h_j\right)^2}\ ,\ l_{ii} = q_{ii} = r_i \\ L_{ij} &= \sqrt{q_{ij}^2 + \left(h_i + h_j\right)^2}\ ,\ L_{ii} = \sqrt{r_i^2 + 4h_i^2} \\ \gamma_2 &= \sqrt{j\omega\mu_2\kappa_2} \simeq \sqrt{j\omega\mu_2\sigma_2} \\ \kappa_2 &= \sigma_2 + j\omega\epsilon_2\,. \end{aligned} \tag{2}$$

The approximation $\gamma_2 \simeq \sqrt{j\omega\mu_2\sigma_2}$ was used in the derivation of the original formulation by Pollaczek. The quantity l_{ij} is the distance between the cable axes, whereas L_{ij} is the distance between cable i and the image of cable j, located symmetrically with respect to the ground–air interface.

Equation (1) may be deduced from the general procedure developed by Sunde [13], starting from the solution of the electromagnetic field in terms of the electric Hertzian potential $\mathbf{\Pi}'$ (Π'_x and Π'_z components), accounting for boundary conditions at the interface between the media at $z = 0$, and including displacement currents in the ground. This approach neglects the effect of propagation along the cable axis (i.e., $\mathrm{e}^{-jk_x x} \simeq 1$) in the derivation of self and mutual elements of the matrix of impedances. The issue is discussed in [18]; Silva et al. [28] demonstrated that, in the case of sea/seabed, k_x is sensibly smaller than γ_m, concluding that the approximation holds with accuracy up to 10 MHz. The impedance $Z'_{2,ij}$ is computed by integration of the electric field (derived from Π'_x) at the axis of cable j, produced by a longitudinally-invariant current I along the axis of cable i. The main issue of this formula is that it has been derived assuming medium 1 as air, and the propagation constant γ_1 is neglected.

After Pollaczek proposed his formula for the ground-return impedances, researchers did not propose any correction to the ground-return admittances, aside from Sunde's development in [13], on the common assumption that it might be neglected (as in ATP/EMTP simulators). For a single cable, the admittance Y'_2 might be approximated as [34] $Y'_2 \simeq \gamma_2^2/Z'_2$.

2) Xue et al.: With respect to the homogeneous earth model in Fig. 2(a), Xue et al. [21] have recently proposed the following formula for the ground-return impedance:

$$Z'_{2,ij} = \frac{j\omega\mu_2}{2\pi}\left[\mathrm{K}_0\left(\gamma_2 l_{ij}\right) - \mathrm{K}_0\left(\gamma_2 L_{ij}\right) + 2\int_0^\infty \frac{\mathrm{e}^{-2\alpha_2 h_{ij}}}{\alpha_1+\alpha_2}\cos\left(\lambda\, q_{ij}\right)\,\mathrm{d}\lambda\right]. \tag{3}$$

The main advantage of this approach, over that of Pollaczek in (1), is in the explicit dependence of the integral in the second term at the right-hand side of (3) on the propagation constant of medium 1 (i.e., on α_1): through suitable manipulation, expression (3) can be adapted to study configurations including seabed–sea interfaces.

As concerns the ground-return admittance matrix $\mathbf{Y}'_2$, it can be computed through inversion of the potential matrix $\mathbf{P}'_2$, as $\mathbf{Y}'_2 = j\omega(\mathbf{P}'_2)^{-1}$ [21], [27]. Xue et al. proposed the following expression for the ground-return potential coefficients:

$$P'_{2,ij} = \frac{j\omega}{2\pi\kappa_2}\left[\mathrm{K}_0\left(\gamma_2 l_{ij}\right) - \mathrm{K}_0\left(\gamma_2 L_{ij}\right) + 2\Delta_5^{\mathrm{QT}} + 2\gamma_2^2\Delta_6^{\mathrm{QT}}\right] \tag{4}$$

where

$$\Delta_5^{\mathrm{QT}} = \int_0^\infty \frac{\mathrm{e}^{-2\alpha_2 h_{ij}}}{\alpha_1 + \left(\frac{\gamma_1}{\gamma_2}\right)^2\alpha_2}\left(\frac{\lambda}{\alpha_2}\right)^2\cos\left(q_{ij}\lambda\right)\,\mathrm{d}\lambda \tag{5a}$$

$$\Delta_6^{\mathrm{QT}} = \int_0^\infty \frac{\mathrm{e}^{-2\alpha_2 h_{ij}}}{\alpha_1+\alpha_1}\frac{1}{\alpha_2^2}\cos\left(q_{ij}\lambda\right)\,\mathrm{d}\lambda\,. \tag{5b}$$

3) Magalhães et al.: Magalhães et al. [23] derived an equivalent formulation to that of Xue et al. for the ground-return impedances. Besides, they revised the formulation of the ground-return admittances and proposed the following expression directly for the ground admittance matrix [22]:

$$\mathbf{Y}_2' = 2\pi\kappa_2 \left(\mathbf{\Lambda} - \mathbf{T}\right)^{-1} \tag{6}$$

where

$$\Lambda_{ij} = \mathrm{K}_0\left(\gamma_2 \mathrm{l_{ij}}\right) - \mathrm{K}_0\left(\gamma_2 \mathrm{L_{ij}}\right) \tag{7a}$$

$$T_{ij} = \int_{-\infty}^{\infty} \frac{\alpha_1}{\alpha_2} \frac{\mathrm{e}^{-\alpha_2 h_{ij}} - \mathrm{e}^{-2\alpha_2 h_{ij}}}{(\gamma_1/\gamma_2)^2 \alpha_2 + \alpha_1} \mathrm{e}^{-j q_{ij}\lambda}\, \mathrm{d}\lambda\,. \tag{7b}$$

4) Papadopoulos et al.: Papadopoulos et al. [18] provided expressions for both ground-return impedances and admittances, following the original theory developed by Sunde [13]. For $Z_{2,ij}'$ the following formula holds:

$$Z_{2,ij}' = \frac{j\omega\mu_2}{2\pi} \int_0^{\infty} F\left(\lambda\right) \cos\left(\lambda q_{ij}\right)\, \mathrm{d}\lambda \tag{8}$$

with

$$F\left(\lambda\right) = \frac{\mathrm{e}^{-\alpha_2 |h_i - h_j|} - \mathrm{e}^{-2\alpha_2 h_{ij}}}{\alpha_2} + \frac{2\mu_1 \mathrm{e}^{-2\alpha_2 h_{ij}}}{\alpha_2 \mu_1 + \alpha_1 \mu_2}\,. \tag{9}$$

In (8)–(9), $\alpha_m = \sqrt{\lambda^2 + \gamma_m^2 + k_x^2}$ with $m = 1$ for air ad $m = 2$ for ground. In addition, k_x is the unknown propagation constant of the mode propagating along the cable in the x-direction (not accounted for in Sunde's and Pollaczeck's derivations). Assuming the approximation $k_x \ll \gamma_m$, the expression coincides with that derived by Sunde [13]. If the additional approximation $\sigma_2 \gg \omega\epsilon_2$ is included, neglecting the displacement currents, Pollaczek's formula is recovered.

The authors proposed also an expression for the potential coefficients

$$P_{2,ij}' = \frac{j\omega}{2\pi\kappa_2} \int_0^{\infty} \left[F\left(\lambda\right) + G\left(\lambda\right)\right] \cos\left(q_{ij}\lambda\right)\, \mathrm{d}\lambda \tag{10}$$

with

$$G\left(\lambda\right) = \frac{2\mu_1\mu_2\alpha_2\left(\gamma_2^2 - \gamma_1^2\right) e^{-2\alpha_2 h_{ij}}}{\left(\alpha_2\mu_1 + \alpha_1\mu_2\right)\left(\alpha_2\gamma_1^2\mu_2 + \alpha_1\gamma_2^2\mu_1\right)}\,. \tag{11}$$

B. Infinite-Sea/Seabed Model

Alternative approaches assume the sea/seabed to extend at infinite distance from the cable. The axial symmetry of the new configuration, where we assume the cables to be placed in a homogenous medium 1 [see Fig. 2(b)] and we neglect the influence of the interfaces between adjacent media, allows a simplified solution of the problem. The solution holds when the penetration depth δ_1 into the surrounding medium (sea or seabed) is much lower than the installation depth h_i (into the sea) or $h_i - h_{\mathrm{s}}$ (into the seabed)

$$\delta_1 = \frac{\sqrt{2}}{|\gamma_1|} \approx \frac{1}{\sqrt{\pi\mu_1}} \frac{1}{\sqrt{f\sigma_1}} \ll h_i, (h_i - h_{\mathrm{s}}) \tag{12}$$

where the surrounding medium is assumed as a good conductor, i.e., for $\sigma_1 \gg \omega\epsilon_1$. The expression of the self-ground-return impedance is derived as an extension of the following formula for coaxial cables derived by Schelkunoff [10]:

$$Z_{1,ii}' = \frac{\gamma_1}{2\pi\sigma_1 r_{\mathrm{in}}} \cdot \frac{\mathrm{I}_0\left(\gamma_1 r_{\mathrm{in}}\right) \mathrm{K}_1\left(\gamma_1 r_{\mathrm{ext}}\right) + \mathrm{K}_0\left(\gamma_1 r_{\mathrm{in}}\right) \mathrm{I}_1\left(\gamma_1 r_{\mathrm{ext}}\right)}{\mathrm{K}_1\left(\gamma_1 r_{\mathrm{in}}\right) I_1\left(\gamma_1 r_{\mathrm{ext}}\right) - \mathrm{I}_1\left(\gamma_1 r_{\mathrm{in}}\right) \mathrm{K}_1\left(\gamma_1 r_{\mathrm{ext}}\right)}. \tag{13}$$

Referring to a generic loop made of two coaxial conductors [10], (13) expresses the p.u.l. impedance offered by the inner surface of the outer conductor of the loop (i.e., sea or seabed), with a radial thickness equal to $r_{\mathrm{ext}} - r_{\mathrm{in}}$. Considering a coaxial arrangement in which the surrounding medium is the external conductor with $r_{\mathrm{in}} = r_i$ and $r_{\mathrm{ext}} \to \infty$, we get

$$Z_{1,ii}' = \frac{\gamma_1}{2\pi\sigma_1 r_i} \frac{\mathrm{K}_0\left(\gamma_1 r_i\right)}{\mathrm{K}_1\left(\gamma_1 r_i\right)}\,. \tag{14}$$

The expression has been generalized to the mutual impedance between the cables [see Fig. 2(b)] [27]

$$Z_{1,ij}' = \frac{1}{2\pi\sigma_1 r_i r_j} \frac{\mathrm{K}_0\left(\gamma_1 l_{ij}\right)}{\mathrm{K}_1\left(\gamma_1 r_i\right) \mathrm{K}_1\left(\gamma_1 r_j\right)}\,. \tag{15}$$

A different expression modeling the infinite-sea return path may be derived by suitable manipulation of the impedance formula (8) by Papadopoulos et al. [18]. Imposing $\gamma_1 = \gamma_2$ in (8), i.e., making equal the two media above and below the interface, we get the following expression:

$$\begin{aligned} Z_{1,ij}' &= \frac{j\omega\mu_1}{2\pi} \int_0^{+\infty} \frac{1}{\sqrt{\lambda^2 + \gamma_1^2}} \cos\left(\lambda\, q_{ij}\right)\, \mathrm{d}\lambda \\ &= \frac{j\omega\mu_1}{2\pi} \frac{1}{2} \int_{-\infty}^{+\infty} \frac{\mathrm{e}^{-j\lambda\, q_{ij}}}{\sqrt{\lambda^2 + \gamma_1^2}}\, \mathrm{d}\lambda = \frac{j\omega\mu_1}{2\pi} \mathrm{K}_0\left(\gamma_1 q_{ij}\right)\,. \end{aligned} \tag{16}$$

Interestingly, the same expression may be obtained also from (15), as an approximation valid in the low-frequency range, and for $\sigma_1 \gg \omega\epsilon_1$

$$\begin{aligned} Z_{1,ij}' &= \frac{1}{2\pi\sigma_1 r_i r_j} \frac{\mathrm{K}_0\left(\gamma_1\, r_i\right)}{\mathrm{K}_1\left(\gamma_1\, r_i\right) \mathrm{K}_1\left(\gamma_1\, r_j\right)} \underset{\gamma_1 \to 0}{\to} \\ &\to \frac{1}{2\pi\sigma_1 r_i r_j} \frac{\mathrm{K}_0\left(\gamma_1\, q_{ij}\right)}{\frac{1}{\gamma_1\, r_i} \frac{1}{\gamma_1\, r_j}} = \frac{\gamma_1^2}{2\pi\sigma_1} \mathrm{K}_0\left(\gamma_1 q_{ij}\right) \\ &\cong \frac{j\omega\mu_1}{2\pi} \mathrm{K}_0\left(\gamma_1 q_{ij}\right)\,. \end{aligned} \tag{17}$$

No approximation is provided for the ground-return admittances, on the assumption that any correction can be neglected.

C. Double-Layer Earth

More advanced approaches account for the three media involved in the study of the p.u.l. impedances/admittances of submarine cables, i.e., air, sea, and seabed (with common electric and magnetic properties listed in Table I). Referring to Fig. 2(c) and (d), we use subscripts 0, 1, and 2 to refer to air, sea, and seabed layers, respectively.

TABLE I
ELECTRIC AND MAGNETIC PROPERTIES OF SEAWATER AND SEABED

	m	ϵ_m [F/m]	σ_m [S/m]	μ_m [H/m]
Air	0	ϵ_0	0	μ_0
Seawater	1	$81\epsilon_0$	5	μ_0
Seabed-type 1	2	$40\epsilon_0$	1.5	μ_0
Seabed-type 2	2	$15\epsilon_0$	0.05	μ_0

1) Tsiamitros et al. and Papadopoulos et al.: Following the Hertzian potential approach used by Sunde, Tsiamitros et al. [19] proposed a formula for the earth-return impedances of two cables placed in layer 1 (i.e., the sea), later generalized by Hemmatian et al. [35] for a three-layer earth, and further developed by Papadopoulos et al. [20], who proposed an expression also for the earth-return admittances in a two-layer earth. According to these models, the p.u.l. impedance of the earth-return path of cables buried in the middle layer 1 [i.e., the sea according to Fig. 2(c)] reads

$$Z'_{1,ij} = \frac{j\omega\mu_1}{2\pi}\int_0^\infty F_1(\lambda)\cos(\lambda q_{ij})\,\mathrm{d}\lambda \tag{18}$$

where

$$\begin{aligned} F_1(\lambda) = &\frac{1}{\alpha_1\left(s_{10}s_{21} - d_{10}d_{21}\mathrm{e}^{-2\alpha_1 h_\mathrm{s}}\right)} \\ &\cdot\Big[s_{10}s_{21}\mathrm{e}^{-\alpha_1|h_i-h_j|} + s_{10}d_{21}\mathrm{e}^{-\alpha_1(2h_\mathrm{s}-h_i-h_j)} \\ &+d_{10}s_{21}\mathrm{e}^{-\alpha_1(h_i+h_j)} + d_{10}d_{21}\mathrm{e}^{-\alpha_1(2h_\mathrm{s}-|h_i-h_j|)}\Big] \end{aligned} \tag{19}$$

and

$$\begin{aligned} s_{10} &= \mu_0\alpha_1 + \mu_1\alpha_0 \quad s_{21} = \mu_2\alpha_1 + \mu_1\alpha_2 \\ d_{10} &= \mu_0\alpha_1 - \mu_1\alpha_0 \quad d_{21} = \mu_2\alpha_1 - \mu_1\alpha_2\,. \end{aligned} \tag{20}$$

For cables immersed into the sea, Papadopoulos et al. [20] proposed an expression for the potential coefficients of the same type as (10) accounting also for the sea–seabed interface

$$P'_{1,ij} = \frac{j\omega}{2\pi\kappa_1}\int_0^\infty \left[F_1(\lambda) + G_\mathrm{s}(\lambda)\right]\cos(q_{ij}\lambda)\,\mathrm{d}\lambda \tag{21}$$

where $G_\mathrm{s}(\lambda)$ is given by

$$G_\mathrm{s}(\lambda) = 2\alpha_1\left[G_1(\lambda) + G_2(\lambda) + G_3(\lambda) + G_4(\lambda)\right]. \tag{22}$$

Expression of the functions G_i with $i = 1, \ldots, 4$ in (22) are given in [20].

2) Lucca: For cables laying in medium 1 and placed on the seabed interface, Lucca [26] derived the following approximated expression for earth-return impedances, working on the expression proposed by Papadopoulos:

$$Z'_{1,ij} \simeq \frac{j\omega\mu_0}{\pi}\int_0^\infty F_2(\lambda)\cos(\lambda q_{ij})\,\mathrm{d}\lambda \tag{23}$$

with

$$F_2(\lambda) = \frac{\alpha_1 + \alpha_0 + (\alpha_1 - \alpha_0)\,\mathrm{e}^{-2\alpha_1 h_i}}{(\alpha_1+\alpha_0)(\alpha_1+\alpha_2) - (\alpha_1-\alpha_0)(\alpha_1-\alpha_2)\,\mathrm{e}^{-2\alpha_1 h_i}}\,. \tag{24}$$

Expression (23) proposed by Lucca is consistent with (18), when $h_i = h_j = h_\mathrm{s}$ (i.e., conductors laying at the same depth over the seabed) and $\mu_1 = \mu_2 = \mu_0$.

III. Proposed Formulation for Cables Buried in the Seabed

In configurations with shallow water, arrangements with the cables buried into the seabed, approximately at 1 m from the seabed interface, are preferred in order to prevent damages by trawling or anchoring activities. We here propose an expression to compute the self and mutual impedances when the cables lay in medium 2, still accounting for the three-layer configuration [see Fig. 2(d)].

The impedance expression is derived by assuming a quasi-TEM propagation mode; the electromagnetic problem can be solved using the electric Hertzian potential $\mathbf{\Pi}'$ as in [18], [19], and [20]. Since the problem is symmetric to the $x-z$ plane, the component Π'_y is null. Introducing the Bessel transform and assuming an electric dipole source placed in the lowest medium 2, the components Π'_x and Π'_z in the three media #0 ($z > h_\mathrm{s}$), #1 ($0 < z < h_\mathrm{s}$) and #2 ($z < 0$) read, respectively

$$\Pi'_{0x} = \int_0^\infty g_0\mathrm{e}^{-\alpha_0(z-h_\mathrm{s})}\mathrm{J}_0(\lambda r)\,\mathrm{d}\lambda \tag{25a}$$

$$\Pi'_{1x} = \int_0^\infty \left[f_1\mathrm{e}^{+\alpha_1(z-h_\mathrm{s})} + g_1\mathrm{e}^{-\alpha_1 z}\right]\mathrm{J}_0(\lambda r)\,\mathrm{d}\lambda \tag{25b}$$

$$\Pi'_{2x} = \int_0^\infty \left[C_i\frac{\lambda}{\alpha_2}\mathrm{e}^{-\alpha_2|z-(h_\mathrm{s}-h_i)|} + f_2\mathrm{e}^{+\alpha_2 z}\right]\mathrm{J}_0(\lambda r)\,\mathrm{d}\lambda \tag{25c}$$

and

$$\Pi'_{0z} = \int_0^\infty \frac{x}{r}q_0\mathrm{e}^{-\alpha_0(z-h_\mathrm{s})}\mathrm{J}_1(\lambda r)\,\mathrm{d}\lambda \tag{26a}$$

$$\Pi'_{1z} = \int_0^\infty \frac{x}{r}\left[p_1\mathrm{e}^{+\alpha_1(z-h_\mathrm{s})} + q_1\mathrm{e}^{-\alpha_1 z}\right]\mathrm{J}_1(\lambda r)\,\mathrm{d}\lambda \tag{26b}$$

$$\Pi'_{2z} = \int_0^\infty \frac{x}{r}p_2\mathrm{e}^{+\alpha_2 z}\mathrm{J}_1(\lambda r)\,\mathrm{d}\lambda\,. \tag{26c}$$

Equations (25) and (26), the quantity α_n is given by $\alpha_n = \sqrt{\lambda^2+\gamma_n^2}$, where $\gamma_n = \sqrt{j\omega\mu_n(\sigma_n + j\omega\epsilon_n)}$ is the propagation constant of the n^{th} medium ($n = 0, 1, 2$) characterized by the constitutive parameters μ_n, σ_n and ϵ_n; in addition, the quantity $r = \sqrt{x^2+y^2}$ is the radial coordinate, and $C_i = \frac{j\omega\mu_2}{4\pi\gamma_2^2}I\mathrm{d}l$ is the constant of the elementary dipole source $I\mathrm{d}l$ placed at h_i below the first interface layer.

The eight unknown functions g_0, f_1, g_1, f_2, q_0, p_1, q_1, and p_2 can be obtained enforcing eight boundary conditions on Π'_x and Π'_z, four at the layer between the horizontal media #0–#1 ($z = h_\mathrm{s}$) and four at the layer between media #1–#2 ($z = 0$), respectively. The four boundary conditions between media m

and n read [18]

$$\gamma_m^2 \Pi'_{mx} = \gamma_n^2 \Pi'_{nx} \tag{27a}$$

$$\frac{\gamma_m^2}{\mu_m}\frac{\partial \Pi'_{mx}}{\partial z} = \frac{\gamma_n^2}{\mu_n}\frac{\partial \Pi'_{nx}}{\partial z} \tag{27b}$$

$$\frac{\gamma_m^2}{\mu_m}\Pi'_{mz} = \frac{\gamma_n^2}{\mu_n}\Pi'_{nz} \tag{27c}$$

$$\frac{\partial \Pi'_{mx}}{\partial x} + \frac{\partial \Pi'_{mz}}{\partial z} = \frac{\partial \Pi'_{nx}}{\partial x} + \frac{\partial \Pi'_{nz}}{\partial z}\ . \tag{27d}$$

Once Π'_{2x} and Π'_{2z} are known, the mutual longitudinal ground impedance $Z'_{2,ij}$ between the source cable i and the observation cable j, assumed of infinite length along the x-axis and both placed in medium #2, is obtained as [19], [35]

$$Z'_{2,ij} = \int_{-\infty}^{\infty} \gamma_2^2 \frac{\Pi'_{2x}\left(z = h_\mathrm{s} - h_j; y = q_{ij}\right)}{I\mathrm{d}l}\,\mathrm{d}x. \tag{28}$$

The integration on the x variable is obtained as in [13], substituting $\int_0^\infty \mathrm{J}_0(\lambda\sqrt{x^2+q_{ij}^2})\mathrm{d}x$ with $\frac{2\cos(\lambda q_{ij})}{\lambda}$. After some straightforward algebra, the final expression of $Z'_{2,ij}$ reads

$$Z'_{2,ij} = \frac{j\omega\mu_2}{2\pi}\int_0^\infty F_3(\lambda)\cos(\lambda q_{ij})\,\mathrm{d}\lambda \tag{29}$$

with

$$F_3(\lambda) = \frac{1}{\alpha_2}\left[\mathrm{e}^{-\alpha_2|h_i-h_j|} - \frac{s_{10}d_{21} - d_{10}s_{21}\mathrm{e}^{-2\alpha_1 h_\mathrm{s}}}{s_{10}s_{21} - d_{10}d_{21}\mathrm{e}^{-2\alpha_1 h_\mathrm{s}}}\mathrm{e}^{-\alpha_2(h_i+h_j-2h_\mathrm{s})}\right]. \tag{30}$$

In (30), the definitions previously given for the auxiliary parameters s_{mn} and d_{mn} in (20) still hold.

For cables buried into the seabed, we propose also a new expression for the potential coefficients, derived through the same approach adopted in [13] and [18]. The potential coefficients $P'_{2,ij}$ can be computed by means of the correction function Q as

$$P'_{2,ij} = \int_{-\infty}^{\infty} \frac{Q\left(z = h_\mathrm{s} - h_j; y = q_{ij}\right)}{I\mathrm{d}l}\,\mathrm{d}x\ . \tag{31}$$

The function Q can be obtained through the following equation:

$$E_{2y} = \frac{\partial}{\partial y}\left[\frac{\partial \Pi'_{2x}}{\partial x} + \frac{\partial \Pi'_{2z}}{\partial z}\right] = \frac{\partial^2 Q}{\partial x \partial y} \tag{32}$$

allowing to derive the final expression of the potential coefficient $P'_{2,ij}$

$$P'_{2,ij} = \frac{j\omega}{2\pi\kappa_2}\int_0^\infty \left[F_3(\lambda) + G_\mathrm{b}(\lambda)\right]\cos(q_{ij}\lambda)\,\mathrm{d}\lambda \tag{33}$$

where $G_\mathrm{b}(\lambda)$ is given by

$$\begin{aligned} G_\mathrm{b}(\lambda) &= 2\mu_1\mu_2\alpha_2\mathrm{e}^{-\alpha_2(h_i+h_j-2h_\mathrm{s})} \\ &\cdot\Big\{\left(\gamma_2^2-\gamma_1^2\right)\left(s_{10}A_{10} - d_{10}\Delta_{10}\mathrm{e}^{-4\alpha_1 h_\mathrm{s}}\right) - 2\mu_0\mu_1\mathrm{e}^{-2\alpha_1 h_\mathrm{s}} \\ &\cdot\left[\alpha_0^2\gamma_1^2\left(\gamma_2^2-\gamma_1^2\right) + \alpha_1^2\gamma_0^2\left(\gamma_2^2+\gamma_1^2\right) - 2\alpha_1^2\gamma_1^2\gamma_2^2\right]\Big\} \end{aligned} \tag{34}$$

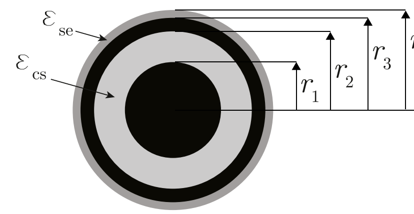

Fig. 3. Layout of the SC cable.

with

$$\begin{aligned} \Delta_{10} &= \alpha_0\gamma_1^2\mu_0 - \alpha_1\gamma_0^2\mu_1 \\ A_{10} &= \alpha_0\gamma_1^2\mu_0 + \alpha_1\gamma_0^2\mu_1\ . \end{aligned} \tag{35}$$

It is worth observing that the first and second terms at the left-hand side in (32) are, respectively, the $F_3(\lambda)$ function in (30) and the $G_\mathrm{b}(\lambda)$ function in (34).

For the two SC cables system considered here, the matrix of p.u.l. potential coefficients $\mathbf{P}'$ is to be found as

$$\mathbf{P}' = \left(\mathbf{T}^t\right)^{-1}\mathbf{P}'_\mathrm{L}\left(\mathbf{T}\right)^{-1}\ . \tag{36}$$

In (36), t denotes the transpose operation.

The matrix $\mathbf{P}'_\mathrm{L}$ is the matrix of p.u.l. potential coefficients referring to loop quantities and is defined as

$$\mathbf{P}'_\mathrm{L} = \begin{bmatrix} P'_\mathrm{cs} & 0 & 0 & 0 \\ 0 & P'_\mathrm{se} + P'_{m,ii} & 0 & P'_{m,ij} \\ 0 & 0 & P'_\mathrm{cs} & 0 \\ 0 & P'_{m,ji} & 0 & P'_\mathrm{se} + P'_{m,jj} \end{bmatrix}. \tag{37}$$

The incidence matrix $\mathbf{T}$ allows us to transform loop quantities to phase quantities (referring to the cables' core and sheath) and it reads

$$\mathbf{T} = \begin{bmatrix} 1 & 0 & 0 & 0 \\ -1 & 1 & 0 & 0 \\ 0 & 0 & 1 & 0 \\ 0 & 0 & -1 & 1 \end{bmatrix}. \tag{38}$$

The interested reader is referred to [36] as concerns the structure of the matrix of potential coefficients of more complex cable layouts and to [27] for the transformation of loop quantities to phase quantities by means of the matrix $\mathbf{T}$.

In (37), P'_cs denotes the p.u.l. potential coefficient associated with the inner insulation, extending between the core and the lead sheath ($r_1 < r < r_2$ in Fig. 3); P'_se denotes the p.u.l. potential coefficient associated with the outer insulation, extending between the lead sheath and the external medium ($r_3 < r < r_4$ in Fig. 3). The two terms are to be computed as

$$P'_\mathrm{cs} = \frac{1}{2\pi\epsilon_\mathrm{cs}}\ln\left(\frac{r_2}{r_1}\right)\ ,\ P'_\mathrm{se} = \frac{1}{2\pi\epsilon_\mathrm{se}}\ln\left(\frac{r_4}{r_3}\right)\ . \tag{39}$$

The self and mutual admittances, Y'_0 and Y'_m, may be derived from the elements of the p.u.l. admittance matrix

$$\mathbf{Y}' = j\omega\left(\mathbf{P}'\right)^{-1}\ . \tag{40}$$

IV. Results and Discussion

Results derived from the implementation of the existing formulations presented in Section II and of the new formulation

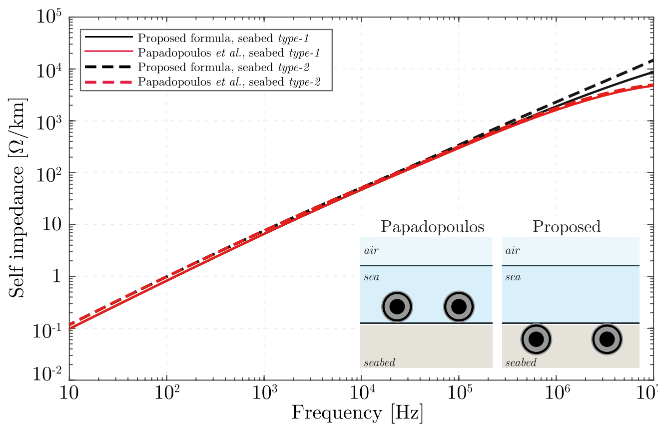

(a)

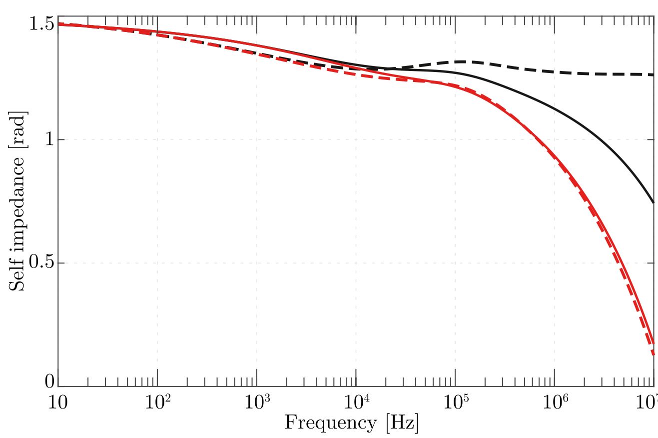

(b)

Fig. 4. Self-impedance of cables laying tangent to the sea–seabed interface for the two different seabed types in Table I ($h_\mathrm{s} = 1$ m). (a) Magnitude. (b) Phase.

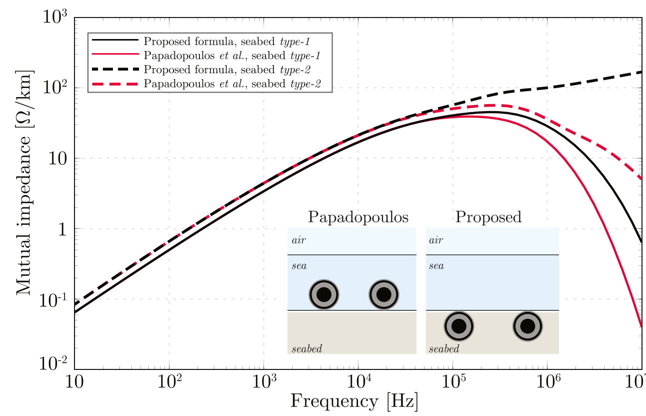

(a)

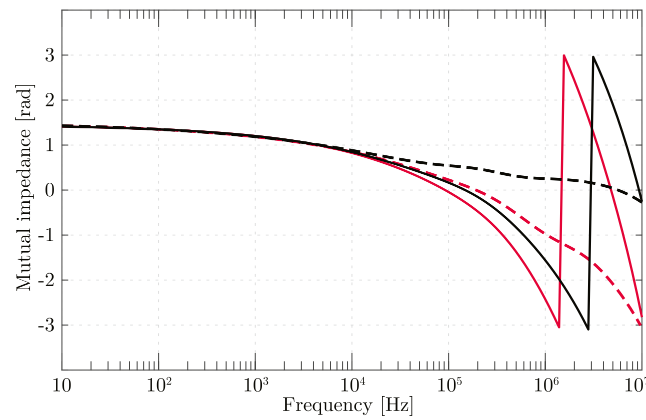

(b)

Fig. 5. Mutual impedance of cables laying tangent to the sea–seabed interface for the two different seabed types in Table I ($h_\mathrm{s} = q_{12} = 1$ m). (a) Magnitude. (b) Phase.

TABLE II
SC CABLE GEOMETRICAL AND PHYSICAL PARAMETERS[1]

	Outer radius	Permittivity	Resistivity
Core	$r_1 = 33.95$ mm	-	$1.7 \cdot 10^{-8}$ Ωm
Inner insulation	$r_2 = 60.65$ mm	$\epsilon_\mathrm{cs} = 3.5\epsilon_0$	-
Lead sheath	$r_3 = 64.65$ mm	-	$21 \cdot 10^{-8}$ Ωm
Outer insulation	$r_4 = 71.05$ mm	$\epsilon_\mathrm{se} = 8\epsilon_0$	-

[1]All layers are to be considered with magnetic permeability μ_0.

proposed in Section III are presented with the seawater and the seabed modeled as homogeneous layers with the electrical and magnetic properties in Table I. Two sets of parameters are adopted to model different seabed types as in [28]. We present results under the assumption $q_{ij} \simeq h_\mathrm{s}$, a common practice adopted by Terna for HVDC submarine cable laying. We consider two SC HVDC cables: the SC cables layout is reported in Fig. 3 and the geometrical/physical parameters are reported in Table II.

We have computed the oscillatory integrals by means of both the double exponential integration technique [37], [38] and the weighted averages algorithm [39] for comparison purpose.

In Figs. 4 and 5, two limiting cases are simulated. First, the self-impedance of cable 1, $Z'_{2,11}$, and the mutual impedance between cables 1 and 2, $Z'_{2,12}$, are computed by the proposed formula when the cables are buried in the seabed (namely, their external surface being tangent to the seabed–water interface), at $h_1 = h_2 = h_\mathrm{s} + r_4$ (see Table II), with $h_\mathrm{s} = q_{12} = 1$ m. Results are compared with $Z'_{1,11}$ and $Z'_{1,12}$ as from (18) by Papadopoulos et al., for $h_1 = h_2 = h_\mathrm{s} - r_4$, for the two seabed types in Table I, and same horizontal distance q_{12} (namely, for the case of cables laying in the water, over the water–seabed interface).

The influence of the seabed electric properties is predominant when computing $Z'_{2,11}$ for cables laying in the seabed. More inductive self-impedances are found for the type-2 seabed, due to its smaller relative permittivity. The actual location of the cable influences its self-impedance noticeably only beyond approximately 10 kHz. Results for mutual terms are comparable in magnitude $|Z'_{1,12}| \simeq |Z'_{2,12}|$ at low frequencies up to 100 kHz, however, above 10 kHz, we observe differences in the phases that are relevant on the type-2 seabed, that is more resistive. In the high-frequency range, above 100 kHz, the difference between the predicted impedances is not negligible, being enhanced for the type-2 seabed due to its small conductivity: the p.u.l. impedance is higher and less inductive.

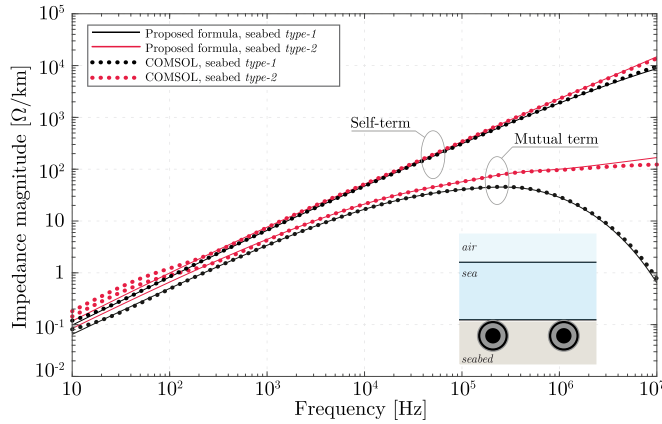

(a)

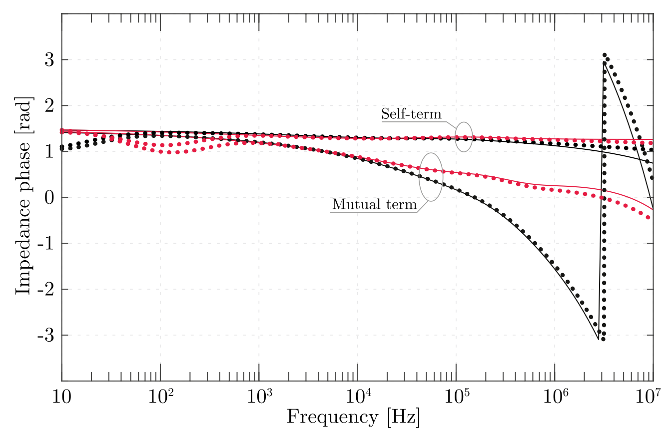

(b)

Fig. 6. Comparison of the p.u.l. impedances $Z'_{2,11}$ and $Z'_{2,12}$ derived by the proposed formula (29) with results computed by COMSOL, with the different seabeds in Table I ($h_s = q_{12} = 1$ m). (a) Magnitude. (b) Phase.

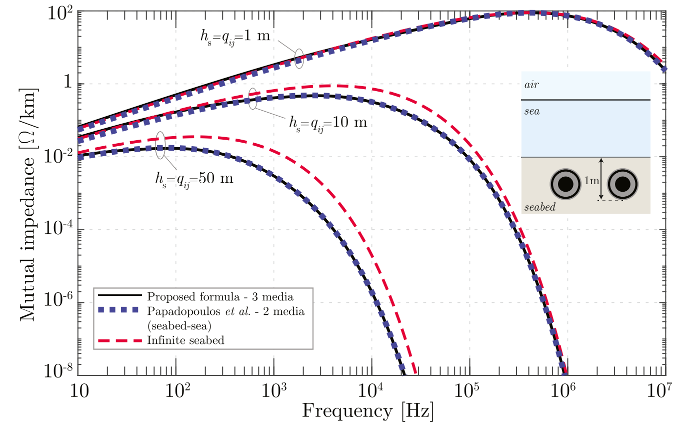

(a)

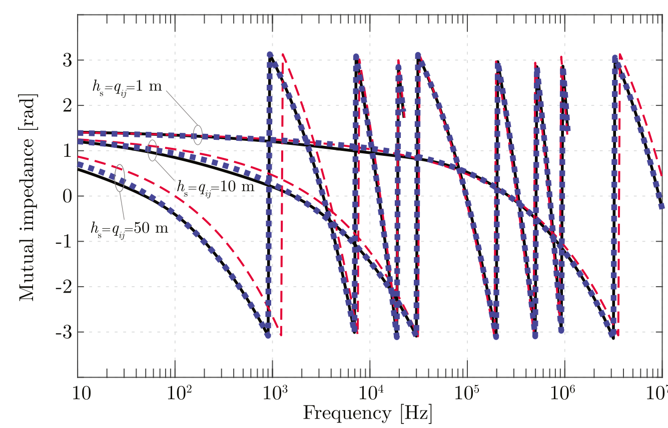

(b)

Fig. 7. Mutual impedance $Z'_{2,12}$ of cables buried in the seabed (type-1) according to different formulations; cables lay at the bottom of a dig in the seabed with depth equal to 1 m. (a) Magnitude. (b) Phase.

Impedances computed by the proposed formula (29) are further compared with results by COMSOL, displayed in Fig. 6, accounting for the double-layer earth. Results are in good agreement in the analyzed range of frequency, the differences observed at low frequencies, approximately below 100 Hz–1 kHz, are due to the truncation with infinite elements of the simulation domain in the finite-element software. Indeed, the accuracy of the infinite elements is a function of the distance from the scatterer at which they are placed, the larger the electromagnetic distance, the higher the infinite elements' ability to simulate the free-field response in the far field. The accuracy of the solution could be improved by moving the infinite-element interface further from the scatterer, leading to higher computational costs. Consequently, it is widely accepted that the performance of infinite elements is less accurate at low frequencies [40].

In Fig. 7, we show the mutual impedance $Z'_{2,12}$ between cables buried in the seabed (1 m below the sea–seabed interface) according to different approximations (we still assume $q_{12} = h_s$). The proposed formula (29) and the formula by Papadopoulos et al. (8), neglecting the third medium (air), give comparable results, both on magnitude and phase: the deviations between the results computed through these two approaches reduce with increasing frequency and for growing depths of the sea layer. The results for $h_s = 10$ m and $h_s = 50$ m are truncated at around 1 MHz and 20 kHz, respectively, due to the low values and loss of precision in the integration. As the values of h_s and q_{12} grow, the mutual impedance becomes smaller, and the two approaches result in negligible deviation. In addition, we observed that the formula by Xue et al. gives results completely superposed on those by Papadopoulos et al. Results computed using an infinite-seabed model [considering the electrical and magnetic properties of the seabed in the place of those typical of the seawater in (14)] are satisfactory when the frequency is higher than 168 kHz according to (12) (considering the burial depth into the seabed equal to 1 m$-r_{\mathrm{ext}}$). At lower frequencies, the effect of the sea layer is relevant, and a single-medium model is not suitable to compute the mutual impedance accurately, especially at high values of q_{12}.

In Fig. 8, we compare the values of the mutual impedance $Z'_{1,12}$ of two cables placed over the seabed (in layer 1—sea) computed utilizing different formulations for several values of sea depth h_s. Results are obtained accounting for the three media as in (18) and accounting only for two semi-infinite layers, i.e., modeling the sea–seabed interface, or the sea–air interface, as

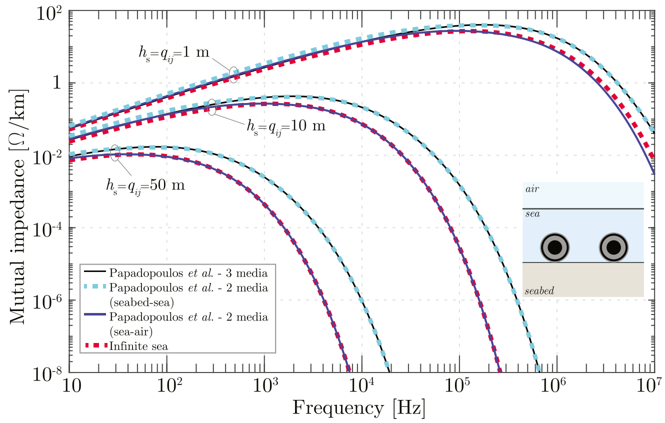

(a)

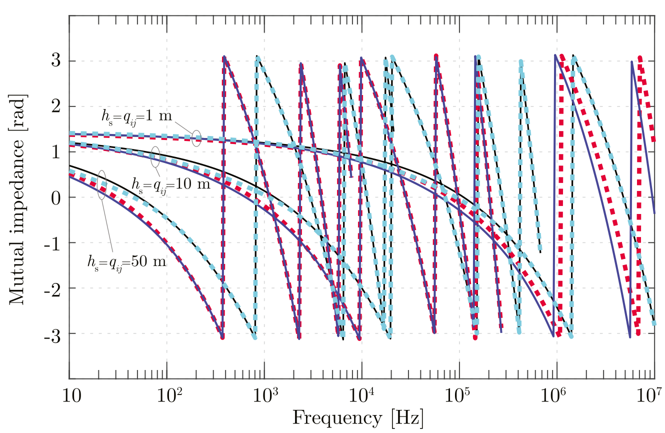

(b)

Fig. 8. Mutual impedance $Z'_{1,12}$ of cables in the sea, laying at the same depth on the seabed–sea interface (seabed type-1). (a) Magnitude. (b) Phase.

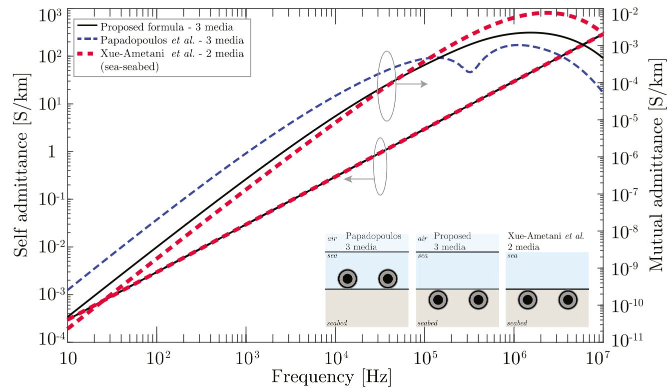

(a)

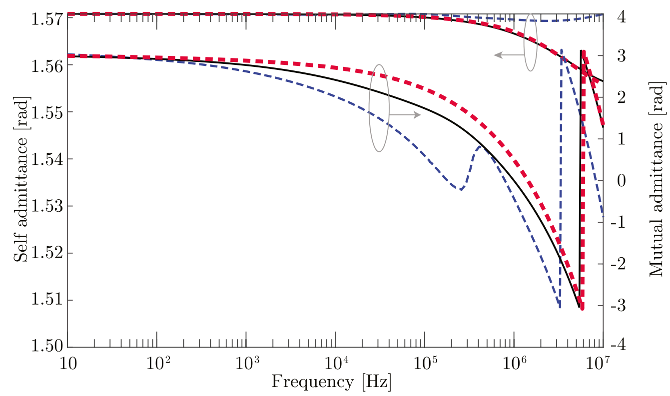

(b)

Fig. 9. Self Y'_0 and mutual Y'_{m} admittances of cables buried into the seabed with $h_{\mathrm{s}} = q_{12} = 1$ m (seabed type-1), considering the effect of the external insulation layer in the potential self-coefficient. (a) Magnitude. (b) Phase.

possible approximate approaches with (8). We also used the approximation of infinite sea. A common observation can be made for the different considered values of h_{s}. Curves computed by the infinite-sea model and by formula (8), written for the sea–air interface, display an excellent agreement over the whole frequency range. Anyway, they do not provide a good approximation since they neglect the seabed interface, which plays a dominant role, being the cables adjacent to it. We can observe the same excellent agreement between the curves obtained through formula (18) (accounting for the three layers) and formula (8) written for the seabed–sea interface. The deviation of the results by the infinite sea and sea–air approximations with respect to the other approaches, accounting also for the seabed–sea interface, is enhanced for increasing values of $h_{\mathrm{s}} = q_{12}$. Hence, the choice of a simplified method to compute the external impedances of cables laying on the seabed should not neglect the influence of the seabed–sea interface, which has a predominant impact on the impedance values.

As concerns the computation of the self and mutual ground admittance parameters Y'_0 and Y'_{m}, it is necessary to compute the whole admittance matrix $\mathbf{Y}'$ of the SC cables from the potential coefficients P'_{ij}. The procedure is addressed in Section III.

Fig. 9 shows the comparison between the self-admittance Y'_0 of the sheath and the mutual admittance Y'_{m} between the sheaths of two cables lying tangent to the sea–seabed interface, above (in the sea) and below (in the seabed) the interface, according to the proposed formula and expressions by Papadopulous et al. for three media, and Xue et al. for two media (sea and seabed). The depth of the sea layer h_{s} and the distance q_{12} between the two cables are equal to 1 m. With reference to (36) and (40), it is possible to observe that the capacitance of the outer insulation layer, introduced through the P'_{se} coefficient, is the dominant term, annihilating or reducing differences in the self and mutual admittance terms, respectively, computed by different formulations. The self-admittance of the sheath is substantially dictated by the outer insulation capacitance, which is much lower than the series-connected capacitance of the ground. From a practical point of view, the sea can be considered a conductive return in the computation of self-admittances.

For the purpose of comparison of the different approaches, we also discuss the self and mutual admittances not considering the effect of the outer insulation layer in Fig. 10 (seabed type-1, $h_{\mathrm{s}} = q_{12} = 1$ m). The formula of Xue et al. provides the same results as that by Papadopulous et al. for two media but its computation is faster. The agreement between the formula proposed in this work and supplied by Xue et al. is acceptable

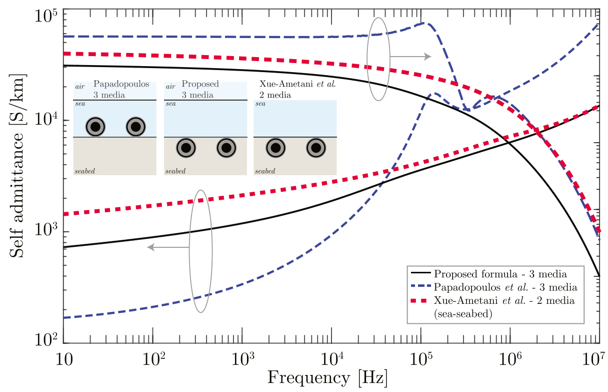

(a)

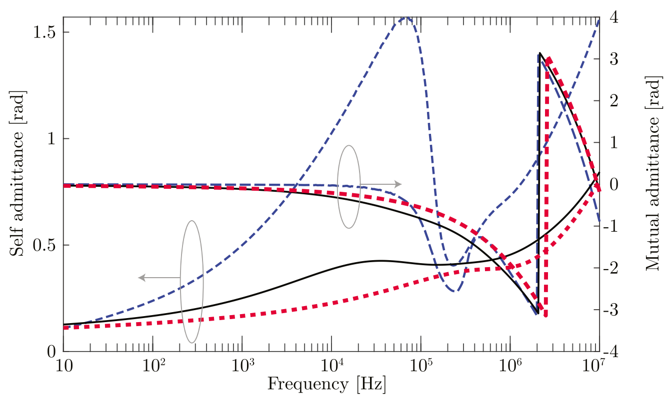

(b)

Fig. 10. Self Y_0' and mutual Y_m' admittances of cables laying tangent to the sea–seabed interface with $h_\mathrm{s} = q_{12} = 1$ m (seabed type-1). (a) Magnitude. (b) Phase.

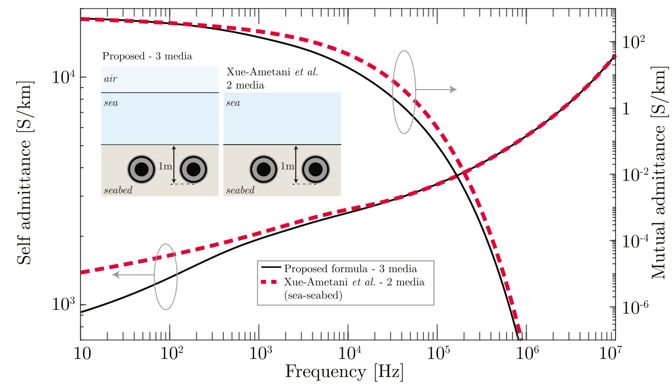

(a)

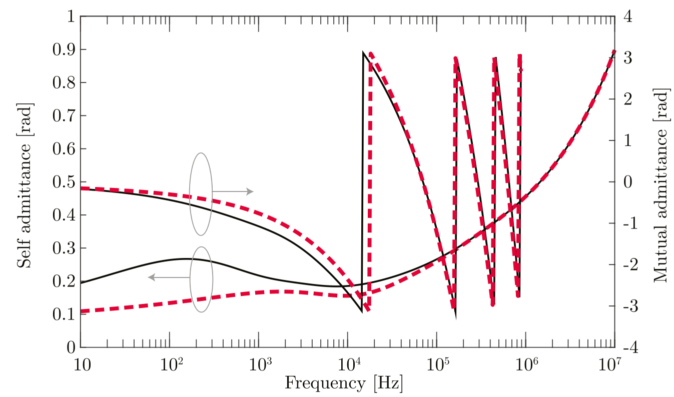

(b)

Fig. 11. Self Y_0' and mutual Y_m' admittances of cables buried into the seabed with $h_\mathrm{s} = q_{12} = 10$ m (seabed type-1). (a) Magnitude. (b) Phase.

at high frequencies, apart from some discrepancies that persist in the phase. It confirms that the sea-air interface plays a neglectable role for sufficiently high frequencies. In addition, the admittance parameters of cables lying in the sea present noticeable differences from those of cables buried in the seabed. Comparing Figs. 5 and 10, we observe that the surrounding medium holds a greater impact on the admittance parameters rather than on the impedance parameters.

The observations are confirmed by Fig. 11, which shows the self and mutual admittances of two cables buried into the seabed 1 m below the interface, with $h_\mathrm{s} = q_{12} = 10$ m. The predictions by the authors agree well with those by Xue et al. above the threshold of 168 kHz, as discussed before, the interface plays a major role at low frequencies. A good agreement with results from COMSOL—not displayed—is obtained only at low frequencies where conductive effects prevail (indeed, the vector magnetic potential is neglected in the computation of the electric field in the adopted Electric Currents physics).

V. Conclusion

This article presents for the first time the expressions of the elements of the p.u.l. ground impedance and admittance matrices of cables buried in the seabed considering a three-layer medium, i.e., air, sea, and seabed. We carried out the computations assuming the low-frequency approximation as in the pioneering work of Sunde, neglecting the propagation constant along the cables. We compared the predictions of the proposed formulas to data obtained through other expressions available in the relevant literature.

The results show that, for practical installation cases, the sea–seabed interface plays a significant role, whereas the air–sea interface can be neglected with excellent accuracy. The two-layer medium approximation (sea and seabed) gave accurate results on the whole frequency range, except for some discrepancies in the admittance parameters at very low frequencies. In the low-frequency range, as far as the penetration depth is higher than the installation depth, the ground impedances of cable laid on the seabed are practically equal to those of cable buried in the seabed. Contrarily, the admittance parameters show higher sensitivity to the surrounding media. The infinite-medium model shows better accuracy as to the approximation of impedances for cables laying in the sea, rather than in the seabed, where it should be used carefully.

Future research will focus on the effect of the p.u.l. ground parameters on the fundamental wave parameters such as characteristic impedances and modal propagation constants of SC cables.

REFERENCES

[1] S. Lauria and F. Palone, "Optimal operation of long inhomogeneous AC cable lines: The Malta-Sicily interconnector," *IEEE Trans. Power Del.*, vol. 29, no. 3, pp. 1036–1044, Jun. 2014.

[2] P. Bresesti, W. L. Kling, R. L. Hendriks, and R. Vailati, "HVDC connection of offshore wind farms to the transmission system," *IEEE Trans. Energy Convers.*, vol. 22, no. 1, pp. 37–43, Mar. 2007.

[3] S. J. Sutton, P. L. Lewin, and S. G. Swingler, "Review of global HVDC subsea cable projects and the application of sea electrodes," *Int. J. Elect. Power Energy Syst.*, vol. 87, pp. 121–135, 2017.

[4] J. Gordonnat and J. Hunt, "Subsea cable key challenges of an intercontinental power link: Case study of Australia-Singapore interconnector," *Energy Transitions*, vol. 4, no. 2, pp. 169–188, 2020.

[5] R. Araneo, J. A. B. Faria, and S. Celozzi, "Frequency-domain analysis of sectionalized shield wires on PLC transmission over high-voltage lines," *IEEE Trans. Electromagn. Compat.*, vol. 99, no. 3, pp. 853–861, Jun. 2017.

[6] E. Stracqualursi, R. Araneo, J. B. Faria, and A. Andreotti, "Application of the transfer matrix approach to direct lightning studies of overhead power lines with underbuilt shield wires—Part I: Theory," *IEEE Trans. Power Del.*, vol. 37, no. 2, pp. 1226–1233, Apr. 2022.

[7] E. Stracqualursi, R. Araneo, J. B. Faria, and A. Andreotti, "Application of the transfer matrix approach to direct lightning studies of overhead power lines with underbuilt shield wires—Part II: Simulation results," *IEEE Trans. Power Del.*, vol. 37, no. 2, pp. 1234–1241, Apr. 2022.

[8] E. Stracqualursi, R. Araneo, P. Burghignoli, G. Lovat, and S. Celozzi, "Unconditionally stable implicit schemes for transient analysis of lossy multiconductor lines," *IEEE Trans. Electromagn. Compat.*, vol. 63, no. 2, pp. 640–644, Apr. 2021.

[9] A. Ametani, Y. Miyamoto, Y. Baba, and N. Nagaoka, "Wave propagation on an overhead multiconductor in a high-frequency region," *IEEE Trans. Electromagn. Compat.*, vol. 56, no. 6, pp. 1638–1648, Dec. 2014.

[10] S. A. Schelkunoff, "The electromagnetic theory of coaxial transmission lines and cylindrical shields," *Bell Syst. Tech. J.*, vol. 13, no. 4, pp. 532–579, 1934.

[11] A. Ametani, "A general formulation of impedance and admittance of cables," *IEEE Trans. Power App. Syst.*, vol. PAS-99, no. 3, pp. 902–910, May 1980.

[12] F. Pollaczek, "Uber das feld einer unendlich langen wechselstrom durch flossen einfachleitung," *Elect. Nachr. Tech.*, vol. 3, no. 9, pp. 339–359, 1926.

[13] E. D. Sunde, *Earth Conduction Effects in Transmission Systems*. Mineola, NY, USA: Dover Pub., Inc., 1968.

[14] R. Araneo and S. Celozzi, "Ground transient resistance of underground cables," *IEEE Trans. Electromagn. Compat.*, vol. 58, no. 3, pp. 931–934, Jun. 2016.

[15] J. R. Wait, "Electromagnetic wave propagation along a buried insulated wire," *Can. J. Phys.*, vol. 50, no. 20, pp. 2402–2409, 1972.

[16] G. E. J. Bridges, "Fields generated by bare and insulated cables buried in a lossy half-space," *IEEE Trans. Geosci. Remote Sens.*, vol. 30, no. 1, pp. 140–146, Jan. 1992.

[17] K. C. Chen, "Transient response of an infinite wire in a dissipative medium," *Interaction Notes on EMP and Related Subjects Dr. C.E. Baum, Editor, IN 453*, 2001.

[18] T. A. Papadopoulos, D. A. Tsiamitros, and G. K. Papagiannis, "Impedances and admittances of underground cables for the homogeneous earth case," *IEEE Trans. Power Del.*, vol. 25, no. 2, pp. 961–969, Apr. 2010.

[19] D. A. Tsiamitros, G. K. Papagiannis, D. P. Labridis, and P. S. Dokopoulos, "Earth return path impedances of underground cables for the two-layer earth case," *IEEE Trans. Power Del.*, vol. 20, no. 3, pp. 2174–2181, Jul. 2005.

[20] T. A. Papadopoulos, D. A. Tsiamitros, and G. K. Papagiannis, "Earth return admittances and impedances of underground cables in non-homogeneous earth," *IET Gener., Transmiss., Distrib.*, vol. 5, no. 2, pp. 161–171, 2011.

[21] H. Xue, A. Ametani, J. Mahseredjian, and I. Kocar, "Generalized formulation of earth-return impedance/admittance and surge analysis on underground cables," *IEEE Trans. Power Del.*, vol. 33, no. 6, pp. 2654–2663, Dec. 2018.

[22] J. P. L. Salvador, A. P. C. Magalhães, A. C. S. Lima, and M. T. Correia de Barros, "Closed-form expression for ground return admittance in underground cables," *IEEE Trans. Power Del.*, vol. 34, no. 6, pp. 2251–2253, Dec. 2019.

[23] A. P. C. Magalhães, M. T. Correia de Barros, and A. C. S. Lima, "Earth return admittance effect on underground cable system modeling," *IEEE Trans. Power Del.*, vol. 33, no. 2, pp. 662–670, Apr. 2018.

[24] A. P. C. Magalhães, A. C. S. Lima, and M. T. Correia de Barros, "Earth return admittance impact on crossbonded underground cables," *Elect. Power Syst. Res.*, vol. 198, 2021, Art. no. 107351.

[25] G. Bianchi and G. Luoni, "Induced currents and losses in single-core submarine cables," *IEEE Trans. Power App. Syst.*, vol. TPAS-95, no. 1, pp. 49–58, Jan. 1976.

[26] G. Lucca, "Evaluation of sea return impedance and mutual impedance between submarine ac power cables and pipelines," *Eur. Trans. Elect. Power*, vol. 21, pp. 273–281, 2011.

[27] R. Benato, M. Forzan, M. Marelli, A. Orini, and E. Zaccone, "Harmonic behaviour of HVDC cables," *Elect. Power Syst. Res.*, vol. 89, pp. 215–222, 2012.

[28] J. C. L. V. Silva, A. C. S. Lima, A. P. C. Magalhães, and M. T. Correia de Barros, "Modeling seabed buried cables for electromagnetic transient analysis," *IET Gener., Transmiss., Distrib.*, vol. 11, pp. 1575–1582, 2017.

[29] U. R. Patel and P. Triverio, "Accurate impedance calculation for underground and submarine power cables using MoM-SO and a multilayer ground model," *IEEE Trans. Power Del.*, vol. 31, no. 3, pp. 1233–1241, Jun. 2016.

[30] T. A. Papadopoulos, Z. G. Datsios, A. I. Chrysochos, P. N. Mikropoulos, and G. K. Papagiannis, "Wave propagation characteristics and electromagnetic transient analysis of underground cable systems considering frequency-dependent soil properties," *IEEE Trans. Electromagn. Compat.*, vol. 63, no. 1, pp. 259–267, Feb. 2021.

[31] T. A. Papadopoulos, Z. G. Datsios, A. I. Chrysochos, P. N. Mikropoulos, and G. K. Papagiannis, "Modal propagation characteristics and transient analysis of multiconductor cable systems buried in lossy dispersive soils," *Elect. Power Syst. Res.*, vol. 196, 2021, Art. no. 107249.

[32] S. Ghosh and S. Das, "A generalized approach to deduce the impedance and admittance of underground cable containing N semiconductor screens," *Eng. Sci. Technol. Int. J.*, vol. 28, 2022, Art. no. 101029.

[33] P. G. A. Njock, Q. Zheng, N. Zhang, and Y.-S. Xu, "Perspective review on subsea jet trenching technology and modeling," *J. Mar. Sci. Eng.*, vol. 8, no. 6, 2020, Art. no. 460.

[34] N. Theethayi, R. Thottappillil, M. Paolone, C. A. Nucci, and F. Rachidi, "External impedance and admittance of buried horizontal wires for transient studies using transmission line analysis," *IEEE Trans. Dielectr. Electr. Insul.*, vol. 14, no. 3, pp. 751–761, Jun. 2007.

[35] B. Hemmatian, B. Vahidi, and S. H. Hosseinian, "Earth return path impedances of underground cable for three-layer earth," *J. Zhejiang Univ.: Sci. A*, vol. 10, no. 8, pp. 1191–1198, 2009.

[36] A. Ametani, T. Ohno, and N. Nagaoka, *Cable System Transients: Theory, Modeling and Simulation*. New York, NY, USA: Wiley, 2015.

[37] T. Ooura and M. Mori, "A robust double exponential formula for Fourier-type integrals," *J. Comput. Appl. Math.*, vol. 112, no. 1–2, pp. 229–241, 1999.

[38] R. Araneo, G. Lovat, P. Burghignoli, and S. Celozzi, "Electromagnetic pulse response of planar screens," *Int. J. Numer. Model. Electron. Netw. Devices Fields*, vol. 31, no. 6, 2018, Art. no. e2329.

[39] R. Golubovic, A. G. Polimeridis, and J. R. Mosig, "Efficient algorithms for computing Sommerfeld integral tails," *IEEE Trans. Antennas Propag.*, vol. 60, no. 5, pp. 2409–2417, May 2012.

[40] R. J. Astley, "Infinite elements for wave problems: A review of current formulations and an assessment of accuracy," *Int. J. Numer. Methods Eng.*, vol. 49, no. 7, pp. 951–976, 2000.

Open Access funding provided by 'Università degli Studi di Roma "La Sapienza" 2' within the CRUI CARE Agreement